







Quantum violation of local causality in an urban network using hybrid photonic technologies

GONZALO CARVACHO,^{1,†} EMANUELE ROCCIA,^{1,†} MAURO VALERI,¹ FRANCESCO BASSO BASSET,¹ DAVIDE PODERINI,¹ CLAUDIO PARDO,¹ EMANUELE POLINO,¹ LORENZO CAROSINI,¹ MICHELE B. ROTA,¹  JULIA NEUWIRTH,¹ SAIMON F. COVRE DA SILVA,² ARMANDO RASTELLI,²  NICOLÒ SPAGNOLO,¹  RAFAEL CHAVES,³ RINALDO TROTTA,^{1,4} AND FABIO SCIARRINO^{1,5} 

¹Dipartimento di Fisica, Sapienza Università di Roma, P.le Aldo Moro 5, I-00185 Roma, Italy

²Institute of Semiconductor and Solid State Physics, Johannes Kepler University, 4040 Linz, Austria

³International Institute of Physics and School of Science and Technology, Federal University of Rio Grande do Norte, 59078-970, P. O. Box 1613, Natal, Brazil

⁴e-mail: rinaldo.trotta@uniroma1.it

⁵e-mail: fabio.sciarrino@uniroma1.it

Received 16 December 2021; revised 31 March 2022; accepted 6 April 2022; published 18 May 2022

Quantum networks play a crucial role in distributed quantum information processing, enabling the establishment of entanglement and quantum communication among distant nodes. Fundamentally, networks with independent sources allow for new forms of nonlocality, beyond the paradigmatic Bell's theorem. Here we implement the simplest of such networks—the bilocality scenario—in an urban network connecting different buildings with a fully scalable and hybrid approach. Two independent sources using different technologies—a quantum dot and a nonlinear crystal—are used to share a photonic entangled state among three nodes connected through a 270 m free-space channel and fiber links. By violating a suitable nonlinear Bell inequality, we demonstrate the nonlocal behavior of the correlations among the nodes of the network. Our results pave the way towards the realization of more complex networks and the implementation of quantum communication protocols in an urban environment, leveraging the capabilities of hybrid photonic technologies. © 2022 Optica Publishing Group under the terms of the [Optica Open Access Publishing Agreement](#)

<https://doi.org/10.1364/OPTICA.451523>

1. INTRODUCTION

In the last decade, several breakthroughs in quantum communication have been reported, especially those regarding the experimental realization of quantum networks [1–4].

Quantum key distribution on fiber networks have demonstrated the possibility to securely connect distances greater than 400 km [5–7], and the successful launch of a satellite allowed the first quantum network covering record distances over 4600 km, integrating space-to-ground and optical fiber communication [8]. At the basis of many of these quantum communication protocols is the phenomenon of Bell nonlocality [9–11], arguably the most radical departure between classical and quantum descriptions of nature. Besides its profound foundational implications, generating nonlocal correlations has become of crucial importance for a variety of quantum technologies, ranging from distributed computing [12], quantum cryptography [13–19] and quantum key distribution [19,20] to randomness generation [21–23] and self-testing [24,25].

Despite the apparent simplicity of Bell's theorem [9], it took over 50 years for the first loophole-free violation of a Bell inequality [26–28]. This has been achieved considering the simplest Bell scenario where a single source distributes entangled pairs between

two distant nodes. Within this context, nonlocal correlations have been obtained using free-space links [29–32], fiber-based links [33–38], and satellite-based communications [38–41]. Moving beyond the paradigmatic Bell scenario, it has been realized that nonlocality can also arise in more complex networks, where the correlations between distant nodes are mediated by a number of independent sources and in a variety of topologies. Motivated by a causality perspective [42], showing in particular that Bell's theorem can be seen as a particular case of a causal inference problem [43,44], quantum networks of growing size and complexity have been attracting increasing theoretical interest [45–58].

In spite of its clear foundational and technological relevance, however, the experimental investigation of these new forms of nonlocality [58–67] has been hampered by difficulties arising from quantum networks.

Indeed, to realize large scale quantum networks and exploit them for practical tasks [4,68], it is crucial to extend their implementation to urban scale scenarios. With that aim, two requirements have to be satisfied: first, the experimental apparatus should be scalable, such that connecting an increasing number of distant nodes is within technological reach; second is the possibility to interface or merge different quantum technologies and types of communication links.

In this work, we take a significant step in this direction, by experimentally realizing a bilocal network [45,46,58,60–62], a scenario akin to the paradigmatic entanglement swapping protocol [69,70]. Importantly, different from previous experiments, we generate nonlocal correlations in this network through a scalable and hybrid photonic platform composed of two photonic sources distributing photons among three nodes. In contrast to implementations that rely on entangled measurements, a demanding task in linear optics [71–73], we exploit separable measurements only, allowing a scalable approach to networks of increasing size. On one hand, separable measurements allow to mix different wavelengths, modes, and technologies, and avoid post-selection, which is necessary for Bell state measurements with linear optics. On the other hand, entangled measurements, while in some cases are needed to make specific claims [74,75], do not offer any advantage to demonstrate the nonlocality in this particular scenario. In this sense, we are taking advantage of the fact that bilocality does not need entangled measurements to be violated or to design a reliable, versatile, and scalable system specifically for that purpose.

Notably, the independent sources of quantum entanglement employ two radically different technologies: spontaneous parametric downconversion (SPDC) and a quantum dot (QD). SPDC is widely used for the generation of polarization entangled photon pairs [76], providing high quality entangled states generated in a compact and cost-effective system. However, its probabilistic generation is a drawback for schemes where post-selection is detrimental. This is the case of achieving an unconditional violation in quantum metrology [77] and avoiding threatening attacks in quantum key distribution [78]. In turn, QDs are a promising platform for realizing deterministic photon sources [79]. The truly hybrid nature of our experiment is further increased by using a fiber-based as well as free-space communication link, arguably the main kinds of communication channels to be used in future urban quantum networks. In particular, the free-space link is a 270 m connection between two buildings in Sapienza University. By violating a Bell inequality suited for the bilocal scenario, we demonstrate the nonlocal nature of the correlations generated among the nodes of the network. This is achieved in the so-called device-independent paradigm [80–85], i.e., without assuming any knowledge of the inner workings of the sources, measurement stations, or other devices. Within the device-independent setting, our experimental demonstration does allow to tackle, at least partially, the locality loophole; however, it relies on the “fair sampling assumption” due to the finite efficiency of the employed detectors. Except for this loophole, which certainly can be addressed by employing more efficient photon detectors, we provide a reliable and versatile platform for an urban quantum network, feasible to be extended to complex scenarios with larger numbers of nodes and sources and covering longer distances.

2. BILOCAL SCENARIO

Bell’s theorem shows that correlations obtained by measurements on distant parties of an entangled system cannot be explained by classical notions of cause and effect. In practice, we impose a given causal structure to our experiment and test whether the constraints arising from a classical description of it, the so-called Bell inequalities, can be violated. The paradigmatic causal structure in Bell’s theorem is shown in Fig. 1(a), represented by a directed acyclic graph (DAG), where each node defines a variable of relevance for the experiment, and the directed edges encode their causal relations. In Bell’s DAG, two distant parties are connected by a single

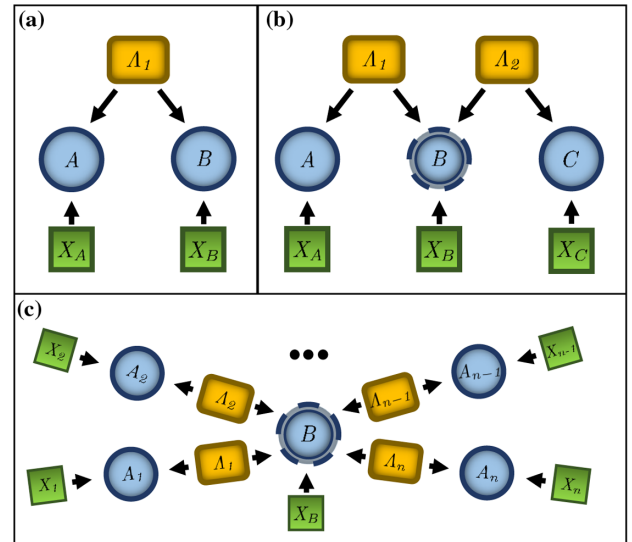


Fig. 1. Directed acyclic graph representation of different causal structures. Examples of network where n -nodes are connected to a central one by means of intermediate nodes, i.e., the star-shaped network (SSN) [62]. (a) Standard Bell scheme. (b) Bilocal scenario. (c) General SSN scheme. Independent sources of correlations ($\Lambda_1, \dots, \Lambda_n$) connect peripheral nodes (A_1, \dots, A_n) to a central one (B). The measurements performed by the nodes are also influenced by their measurement choices (X_B, X_1, \dots, X_n). In particular, central node B consists of different measurement setups that are influenced by different sources, $\Lambda_1, \dots, \Lambda_n$, and the same measurement choice X_B .

source, classically described by a hidden variable Λ , generating the correlations between measurement outcomes A and B given that the parties measure observables parametrized by X_A and X_B , respectively.

It has been realized that networks of different topologies involving an increasing number of nodes and independent sources can lead to new forms of nonlocality [46,48–58], motivating several experimental implementations [58–67]. In particular, the bilocality scenario provides the simplest network beyond the bipartite case and for this reason has attracted significant interest [45–48,58–62]. Its causal structure is represented in Fig. 1(b), where two nodes (A, C) are connected with a central one (B), by means of two independent sources of correlations (Λ_1, Λ_2) [86]. In each node (A, B, C), an observer freely and independently chooses an observable to measure according to a choice (x_A, x_B, x_C), obtaining the outcome (a, b, c), respectively.

The classical description of the bilocal scenario is uniquely defined by the Markov condition [42], which constrains the conditional probabilities of the measurement outcomes as

$$p(a, b, c | x_A, x_B, x_C) = \sum_{\lambda_1, \lambda_2} p(\lambda_1) p(\lambda_2) \times p(a | x_A, \lambda_1) p(c | x_C, \lambda_2) p(b | x_B, \lambda_1, \lambda_2), \quad (1)$$

in which the independence of the sources implies the nonlinear condition $p(\lambda_1, \lambda_2) = p(\lambda_1) p(\lambda_2)$. If one out of two possible dichotomic measurements is performed, i.e., $a, b, c \in \{0, 1\}$ and $x_A, x_B, x_C \in \{0, 1\}$, the classical description (1) implies that the observed correlations should respect a nonlinear Bell inequality given by [45,46,50,51,87]

$$\mathcal{B} = \sqrt{|I_1|} + \sqrt{|I_2|} \leq 1, \quad (2)$$

where

$$I_1 = \frac{1}{4} \sum_{x_A, x_C} \langle A^{x_A} B^0 C^{x_C} \rangle,$$

$$I_2 = \frac{1}{4} \sum_{x_A, x_C} (-1)^{x_A + x_C} \langle A^{x_A} B^1 C^{x_C} \rangle,$$

$$\langle A^{x_A} B^{x_B} C^{x_C} \rangle = \sum_{a, b, c} (-1)^{a+b+c} p(a, b, c | x_A, x_B, x_C). \quad (3)$$

The quantum description of the bilocal experiment involves two sources represented by bipartite quantum states ρ_1, ρ_2 and the measurements given by the operators $\hat{A}^{x_A}, \hat{B}^{x_B}, \hat{C}^{x_C}$ acting on their respective subsystem. The corresponding measurement correlations are given by the Born's rule $\langle A^{x_A} B^{x_B} C^{x_C} \rangle = \text{Tr}[(\hat{A}^{x_A} \otimes \hat{B}^{x_B} \otimes \hat{C}^{x_C})(\rho_1 \otimes \rho_2)]$. As demonstrated by previous works [58–61], when properly choosing the quantum states and measurements, the bilocality inequality (2) can be violated, showing the incompatibility between classical causality and quantum predictions also in this new kind of causal network.

Remarkably, separable measurements in central node B also allows to violate such inequalities [46,60,62,88,89]. In particular, when singlet quantum states, $|\Psi_1^-\rangle$ and $|\Psi_2^-\rangle$, are prepared by the two sources and distributed between the parties, a maximum violation of the bilocal Bell-like inequality can be obtained: $B_Q^{\max} = \sqrt{2} \approx 1.414$. This value is achieved by considering two separable observables in central node B that measure the single-qubit subsystems of the singlet state shared with A and C : $\hat{B}^{x_B} = \hat{B}_A^{x_B} \otimes \hat{B}_C^{x_B}$. Both observables can be taken as Pauli matrices σ_z and σ_x , while each of the external nodes measures

$(\sigma_x + \sigma_z)/\sqrt{2}$ and $(\sigma_x - \sigma_z)/\sqrt{2}$. Separable measurements are particularly suitable to guarantee the scalability of the network, since it can be implemented using independent photonic platforms without the stringent and expensive requirements needed to perform entangled measurements. This is precisely our case, since we even adopt different quantum emitters of single photons, a SPDC source and a QD pumped by independent lasers working in continuous and pulsed modes, respectively. Importantly, the violation of the bilocality inequality (2) is possible even if the distribution $p(a, b, c | x_A, x_B, x_C)$ does not violate any standard Bell inequality. For instance, the choices of states and measurements described above and that will be used in our experimental implementation cannot violate the Clauser–Horne–Shimony–Holt (CHSH) inequality [90] between stations A and B , given by

$$S_{AB} = \sum_{x_A, x_B} (-1)^{x_A x_B} \langle A^{x_A} B^{x_B} \rangle \leq 2, \quad (4)$$

and similarly cannot violate the corresponding CHSH inequality between stations B and C . That is, the non-classicality of the considered statistics truly requires the test of the underlying bilocality network to be detected.

3. EXPERIMENTAL APPARATUS

In the following, we discuss the photonic platform implementing the bilocality network and achieving the violation of inequality (2); see Fig. 2 for details.

One of the sources (ρ_1) of polarization-entangled photons consists of a single GaAs/Al_{0.4}Ga_{0.6}As QD. The QDs are fabricated

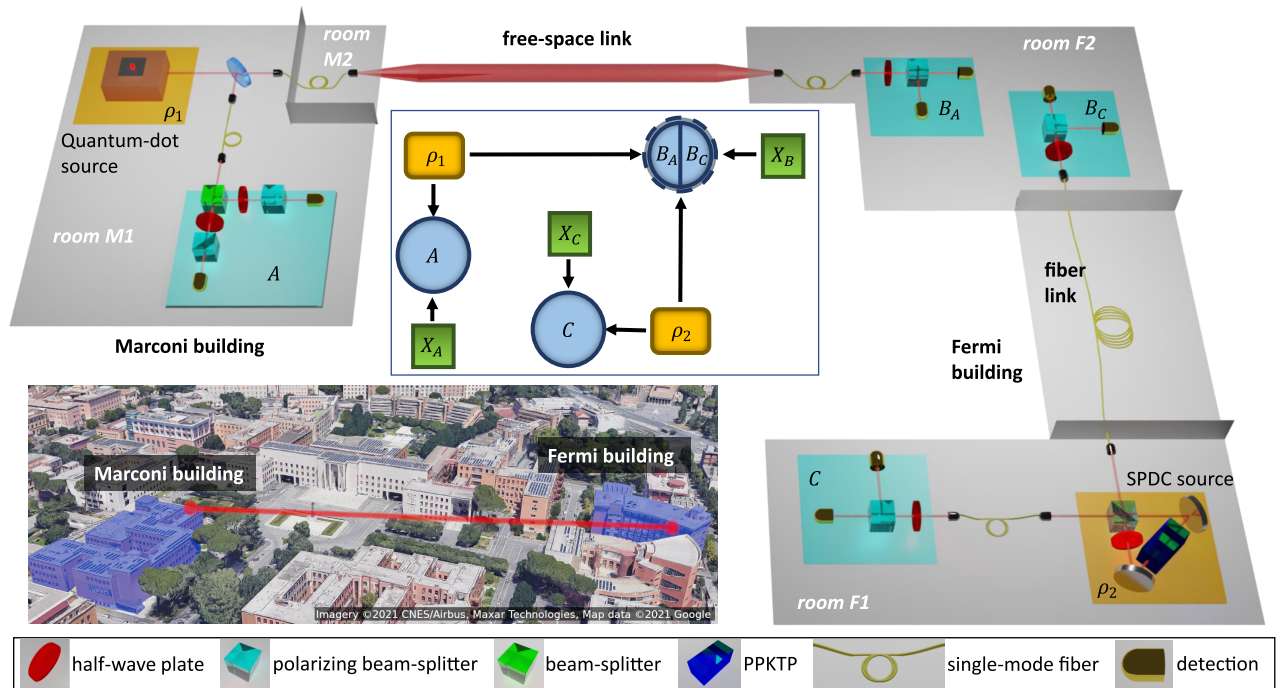


Fig. 2. Experimental implementation of the quantum network. To realize the bilocal scenario, multiple laboratories located in different rooms and buildings were used. In particular, two sources of polarization-entangled photon pairs are realized via a QD device and SPDC in a Sagnac interferometer. They are placed inside the laboratories of two different buildings, respectively, the Marconi and Fermi buildings. The entanglement is distributed from such laboratories to a central one—placed in the Fermi building—by using a free-space channel and a fiber link. A dedicated stabilization system was employed to use the free-space link (not shown in the figure). The corresponding bilocal scheme in DAG representation is reported in the middle: according to Fig. 1(b), two independent sources of correlations (ρ_1, ρ_2) connect two external nodes (A, C) to a central one (B). The two measurement setups connected to the different sources are indicated as B_A and B_C .

with the Al droplet etching method [91] and placed between two asymmetric distributed Bragg reflectors, as detailed in [92]. Using a Weierstrass solid immersion lens and an aspheric lens for collection, the extraction efficiency is approximately 10%. The QD is pumped under resonant two-photon excitation [93] at 782.2 nm with a laser repetition rate of 320 MHz. The rate of measured coincidence events at the source output is 13.7 kHz. The QD with a low fine-structure splitting (FSS) of $0.8 \pm 0.5 \mu\text{eV}$ is selected to achieve a measured fidelity to a maximally entangled state of 0.929 ± 0.004 , without the need for temporal or spectral filtering. After rotating the photon pair onto the singlet state of polarization using a set of wave plates, the measured CHSH parameter (4) is $S_{\text{QD}} = 2.66 \pm 0.02$.

Regarding the SPDC source (ρ_2), entangled photon pairs are generated pumping a nonlinear ppKTP crystal [94] placed into a Sagnac interferometer. The continuous-wave pump has a frequency of 405 nm, while the signal-idler generation is degenerate at 810 nm. The rate of measured coincidence events between the two output modes is 3 kHz, generating a singlet state $|\Psi^-\rangle$ (with a fidelity equal to 0.955 ± 0.001) able to violate the CHSH inequality $S_{\text{SPDC}} = 2.727 \pm 0.007$. In addition, the source is mounted in a compact and monolithic architecture (see Supplement 1) providing high signal stability, as well as enabling the possibility to transfer and operate the source in different locations.

Using these sources of photonic entanglement, the implemented quantum bilocal network is reported in Fig. 2. The source $\rho_1(\rho_2)$ is shared between the external node $A(C)$ and the central one (B). Both sources are located near the corresponding peripheral nodes, i.e., source $\rho_1(\rho_2)$ is in the same laboratory as measurement station $A(C)$. Two stations, B and C , are placed in two distinct laboratories inside the same building, and are connected through a 25 m long single-mode fiber. The other station A is placed in a different building 270 m apart from the one of B and C . This node is connected to the central one (B) through a free-space channel stabilized by a dedicated system using the feedback from an additional reference laser at 850 nm and a couple of piezoelectric mirrors at the receiver to counter the effects of atmospheric turbulence and beam wander [32], plus a piezoelectric mirror at the sender to remove thermal drifts in the pointing direction (see Supplement 1). To realize optimal measurements, each station is equipped with standard setups for linear polarization measurement (see Supplement 1).

4. RESULTS

Each observable of the tripartite system ABC requires the simultaneous detection of four-fold coincidence events. To achieve this, we first record two-fold events of subsystems AB and BC, independently. Then, four-fold events are recovered by filtering all the two-fold data inside a given time window. This procedure allows us to considerably reduce background noise while retaining an optimal rate for the four-fold events. The size of the window can be tuned, thus varying the statistics and the considered simultaneity of the events, similar to [62]. The analysis of the violation of Eq. (2) is reported in Fig. 3, where optimal performances are reached for the window 51.44 μs . Using this window, we obtain a mean value of $\mathcal{B}_{\text{exp}} = 1.312 \pm 0.0052$ averaged over ~ 25 min. Further, two-fold events can be processed to extract the values of Bell parameters distributed along the quantum channels during the bilocal experiment. The analysis provides CHSH violations of $S_{AB} = 2.484 \pm 0.018$ and $S_{BC} = 2.699 \pm 0.006$ for the signal

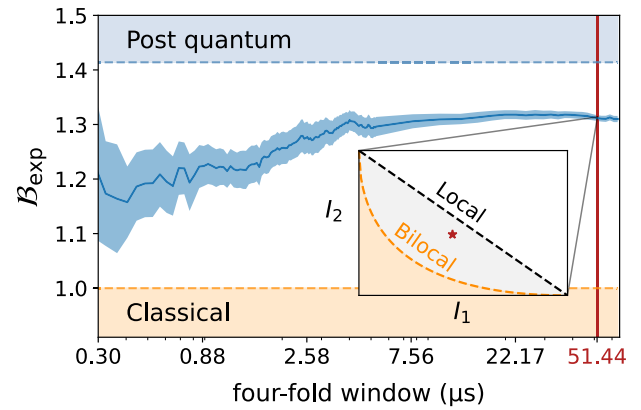


Fig. 3. Experimental results. Quantum violation \mathcal{B}_{exp} is shown as a function of the time window in which four-fold coincidence events are considered simultaneous. The dashed orange and blue lines represent classical and the quantum bounds, $\mathcal{B}_{\text{cl}} = 1$ and $\mathcal{B}_Q = \sqrt{2}$, respectively, so that the orange region defines the values of \mathcal{B} allowed by classical models, while the blue one, i.e., the post-quantum region, is inaccessible even with quantum resources (the logical maximum of $\mathcal{B}_{\text{PR}} = 2$ is reached, in principle, only by no-signaling distributions like a Popescu–Rohrlich box [95]). The solid blue line indicates the measured value of \mathcal{B}_{exp} with the corresponding error represented by the light blue area. The error is computed through repeated measurements over ~ 25 min. While the optimal value, in terms of σ -distance from the bound, is reached using a window of 51.44 μs , a significant violation can be obtained also considering much smaller windows, up to 0.30 μs . In the inset, the point corresponding to the optimal window of 51.44 μs is shown in the space of correlations I_1, I_2 , as defined in Eq. (3), where the classical bound corresponding the bilocal scenario is represented by the orange area, while the gray area represents the classical correlations allowed by the relaxed scenario in which the assumption of independence of the source is lifted, corresponding to a tripartite Bell scenario.

coming from the QD and the SPDC source, respectively. The time trend of CHSH and bilocal violation of our network can be found in Supplement 1. Notably, we obtain a violation of the classical limit also with windows in the range 300–800 ns, which, in principle, allows the events in nodes A and B to be recorded with space-like separations with respect to C , partially addressing the locality loophole of our implementation.

5. CONCLUSION

A crucial requirement for the development of quantum communication networks is the ability to exploit and combine widely different technologies that are currently available, in a modular and reliable way. In this direction, we experimentally demonstrate the quantum violation of local causality in a hybrid tripartite quantum network. We violate a bilocal inequality, surpassing the classical bound by more than 60 standard deviations and thus prove the emergence of nonclassical correlations that cannot be detected by standard Bell inequalities. Our network is composed of three nodes interconnected by fiber and free-space photonic links and two distinct sources of entangled photons. The two sources are based on significantly different technologies: SPDC-based generation at 810 nm pumped by a 405 nm continuous-wave laser and QD emission at 781.2–783.2 nm pumped in pulsed regime. Thus, our platform employs two intrinsically independent sources, a fundamental requirement for testing classical bounds in networks such as the bilocal scenario and others of increasing size and number

of sources. Furthermore, we studied the violation of the Bell-like inequality for such a scenario, tuning the time window in which four-fold coincidence events are considered simultaneous, including time windows in which the events in the distant stations can be considered space-like separated, an important ingredient for a fully loophole-free demonstration. This work shows the reliability and versatility of the implemented platform, merging and interfacing technologically different solutions in the same network. The use of separable measurements allows interfacing sources of different natures, avoiding the drawbacks of optical Bell-state measurements requiring also the synchronization of single-photon emission [96]. Furthermore, our experiment has employed both free-space and fiber links in an urban environment, whose combined adoption represents a crucial requirement towards large scale networks. All these features demonstrate that our approach can be easily applied and scaled to any complex causal network, and can be used as a building block for future real-life quantum secure communication networks based on quantum nonlocality.

Funding. LIT Secure and Correct Systems Lab, supported by the State of Upper Austria and the Austrian Science Fund (FWF) Research group FG5; Linz Institute of Technology; Horizon 2020 Framework Programme (871130, 899814); Conselho Nacional de Desenvolvimento Científico e Tecnológico (307172/2017-1, 311375/2020-0); Instituto Serrapilheira (Serra-1708-15763); John Templeton Foundation (61084, 61466); Ministero dell'Istruzione, dell'Università e della Ricerca (2017SRNBRK); European Research Council (679183); Avvio alla ricerca tipo II (AR21916B86E161CE).

Acknowledgment. This work was financially supported by the European Research Council (ERC) under the European Union's Horizon 2020 Research and Innovation Programme (SPQRel), and by MIUR (Ministero dell'Istruzione, dell'Università e della Ricerca) via project PRIN 2017 "Taming complexity via QUantum Strategies a Hybrid Integrated Photonic approach" (QUSHIP). We acknowledge support from The John Templeton Foundation via the grant, the Quantum Information Structure of Spacetime (QISS) Project (qiss.fr) (the opinions expressed in this publication are those of the authors and do not necessarily reflect the views of The John Templeton Foundation). This project has received funding from the European Union's Horizon 2020 Research and Innovation Program (Quoore) (Ascent+). RC also acknowledges the Serrapilheira Institute, the Brazilian National Council for Scientific and Technological Development (CNPq) via the INCT-IQ. G.C. also acknowledges the project "Avvio alla ricerca tipo II" Prot. AR21916B86E161CE.

Disclosures. The authors declare no conflicts of interest.

Data availability. Data may be obtained from the authors upon reasonable request.

Supplemental document. See Supplement 1 for supporting content.

[†]These authors contributed equally to this work.

REFERENCES

- N. Gisin and R. Thew, "Quantum communication," *Nat. Photonics* **1**, 165–171 (2007).
- H.-K. Lo, M. Curty, and K. Tamaki, "Secure quantum key distribution," *Nat. Photonics* **8**, 595–604 (2014).
- E. Diamanti, H.-K. Lo, B. Qi, and Z. Yuan, "Practical challenges in quantum key distribution," *npj Quantum Inf.* **2**, 1–12 (2016).
- S. Wehner, D. Elkouss, and R. Hanson, "Quantum internet: a vision for the road ahead," *Science* **362**, eaam9288 (2018).
- J.-P. Chen, C. Zhang, Y. Liu, C. Jiang, W. Zhang, X.-L. Hu, J.-Y. Guan, Z.-W. Yu, H. Xu, and J. Lin, "Sending-or-not-sending with independent lasers: secure twin-field quantum key distribution over 509 km," *Phys. Rev. Lett.* **124**, 070501 (2020).
- A. Boaron, G. Boso, D. Rusca, C. Vulliez, C. Autebert, M. Caloz, M. Perrenoud, G. Gras, F. Bussi eres, M.-J. Li, D. Nolan, A. Martin, and H. Zbinden, "Secure quantum key distribution over 421 km of optical fiber," *Phys. Rev. Lett.* **121**, 190502 (2018).
- H.-L. Yin, T.-Y. Chen, Z.-W. Yu, H. Liu, L.-X. You, Y.-H. Zhou, S.-J. Chen, Y. Mao, M.-Q. Huang, and W.-J. Zhang, "Measurement-device-independent quantum key distribution over a 404 km optical fiber," *Phys. Rev. Lett.* **117**, 190501 (2016).
- Y.-A. Chen, Q. Zhang, T.-Y. Chen, *et al.*, "An integrated space-to-ground quantum communication network over 4,600 kilometres," *Nature* **589**, 214–219 (2021).
- J. S. Bell, "On the Einstein Podolsky Rosen paradox," *Phys. Phys. Fizika* **1**, 195 (1964).
- N. Brunner, D. Cavalcanti, S. Pironio, V. Scarani, and S. Wehner, "Bell nonlocality," *Rev. Mod. Phys.* **86**, 419 (2014).
- V. Scarani, *Bell Nonlocality* (Oxford University, 2019).
- H. Buhrman, R. Cleve, S. Massar, and R. de Wolf, "Nonlocality and communication complexity," *Rev. Mod. Phys.* **82**, 665–698 (2010).
- N. Gisin, G. Ribordy, W. Tittel, and H. Zbinden, "Quantum cryptography," *Rev. Mod. Phys.* **74**, 145–195 (2002).
- A. K. Ekert, "Quantum cryptography based on Bell's theorem," *Phys. Rev. Lett.* **67**, 661–663 (1991).
- T. Jennewein, C. Simon, G. Weihs, H. Weinfurter, and A. Zeilinger, "Quantum cryptography with entangled photons," *Phys. Rev. Lett.* **84**, 4729–4732 (2000).
- C. Schimpf, M. Reindl, D. Huber, B. Lehner, S. F. Covre da Silva, M. Vyvlecka, P. Walther, and A. Rastelli, "Quantum cryptography with highly entangled photons from semiconductor quantum dots," *Sci. Adv.* **7**, eabe8905 (2021).
- V. Scarani, H. Bechmann-Pasquinucci, N. J. Cerf, M. Dušek, N. Lütkenhaus, and M. Peev, "The security of practical quantum key distribution," *Rev. Mod. Phys.* **81**, 1301 (2009).
- F. Xu, X. Ma, Q. Zhang, H.-K. Lo, and J.-W. Pan, "Secure quantum key distribution with realistic devices," *Rev. Mod. Phys.* **92**, 025002 (2020).
- J. Barrett, L. Hardy, and A. Kent, "No signaling and quantum key distribution," *Phys. Rev. Lett.* **95**, 010503 (2005).
- A. Acn, N. Gisin, and L. Masanes, "From Bell's theorem to secure quantum key distribution," *Phys. Rev. Lett.* **97**, 120405 (2006).
- S. Pironio, A. Acín, S. Massar, A. Boyer de la Giroday, D. N. Matsukevich, P. Maunz, S. Olmschen, D. Hayes, L. Luo, T. A. Manning, and C. Monroe, "Random numbers certified by Bell's theorem," *Nature* **464**, 1021–1024 (2010).
- Y. Liu, Q. Zhao, M.-H. Li, J.-Y. Guan, Y. Zhang, B. Bai, W. Zhang, W.-Z. Liu, C. Wu, X. Yuan, H. Li, W. J. Munro, Z. Wang, L. You, J. Zhang, X. Ma, J. Fan, Q. Zhang, and J.-W. Pan, "Device-independent quantum random-number generation," *Nature* **562**, 548–551 (2018).
- I. Agresti, D. Poderini, L. Guerini, M. Mancusi, G. Carvacho, L. Aolita, D. Cavalcanti, R. Chaves, and F. Sciarrino, "Experimental device-independent certified randomness generation with an instrumental causal structure," *Commun. Phys.* **3**, 110 (2020).
- I. Šupić and J. Bowles, "Self-testing of quantum systems: a review," *Quantum* **4**, 337 (2020).
- I. Agresti, B. Polacchi, D. Poderini, E. Polino, A. Suprano, I. Šupić, J. Bowles, G. Carvacho, D. Cavalcanti, and F. Sciarrino, "Experimental robust self-testing of the state generated by a quantum network," *PRX Quantum* **2**, 020346 (2021).
- M. Giustina, M. A. M. Versteegh, S. Wengerowsky, *et al.*, "Significant-loophole-free test of Bell's theorem with entangled photons," *Phys. Rev. Lett.* **115**, 250401 (2015).
- L. K. Shalm, E. Meyer-Scott, B. G. Christensen, *et al.*, "Strong loophole-free test of local realism," *Phys. Rev. Lett.* **115**, 250402 (2015).
- B. Hensen, H. Bernien, A. E. Dr eau, A. Reiserer, N. Kalb, M. S. Blok, J. Ruitenberg, R. F. L. Vermeulen, R. N. Schouten, C. Abell an, W. Amaya, V. Pruneri, M. W. Mitchell, M. Markham, D. J. Twitchen, D. Elkouss, S. Wehner, T. H. Taminiau, and R. Hanson, "Loophole-free Bell inequality violation using electron spins separated by 1.3 kilometres," *Nature* **526**, 682–686 (2015).
- C.-Z. Peng, T. Yang, X.-H. Bao, J. Zhang, X.-M. Jin, F.-Y. Feng, B. Yang, J. Yang, J. Yin, Q. Zhang, N. Li, B.-L. Tian, and J.-W. Pan, "Experimental free-space distribution of entangled photon pairs over 13 km: towards satellite-based global quantum communication," *Phys. Rev. Lett.* **94**, 150501 (2005).
- X.-S. Ma, T. Herbst, T. Scheidl, D. Wang, S. Kropatschek, W. Naylor, B. Wittmann, A. Mech, J. Kofler, E. Anisimova, V. Makarov, T. Jennewein, R. Ursin, and A. Zeilinger, "Quantum teleportation over 143 kilometres using active feed-forward," *Nature* **489**, 269–273 (2012).
- J. Yin, J.-G. Ren, H. Lu, Y. Cao, H.-L. Yong, Y.-P. Wu, C. Liu, S.-K. Liao, F. Zhou, Y. Jiang, X.-D. Cai, P. Xu, G.-S. Pan, J.-J. Jia, Y.-M. Huang, H. Yin,

- J.-Y. Wang, Y.-A. Chen, C.-Z. Peng, and J.-W. Pan, "Quantum teleportation and entanglement distribution over 100 kilometre free-space channels," *Nature* **488**, 185–188 (2012).
32. F. Basso Basset, M. Valeri, E. Roccia, V. Muredda, D. Poderini, J. Neuwirth, N. Spagnolo, M. B. Rota, G. Carvacho, F. Sciarrino, and R. Trotta, "Quantum key distribution with entangled photons generated on demand by a quantum dot," *Sci. Adv.* **7**, eabe6379 (2021).
 33. S. Wengerowsky, S. K. Joshi, F. Steinlechner, J. R. Zichi, S. M. Dobrovolskiy, R. van der Molen, J. W. N. Los, V. Zwiller, M. A. M. Versteegh, A. Mura, D. Calonico, M. Inguscio, H. Hübel, L. Bo, T. Scheidl, A. Zeilinger, A. Xuereb, and R. Ursin, "Entanglement distribution over a 96-km-long submarine optical fiber," *Proc. Natl. Acad. Sci. USA* **116**, 6684–6688 (2019).
 34. T. Ikuta and H. Takesue, "Four-dimensional entanglement distribution over 100 km," *Sci. Rep.* **8**, 817 (2018).
 35. J. F. Dynes, H. Takesue, Z. L. Yuan, A. W. Sharpe, K. Harada, T. Honjo, H. Kamada, O. Tadanaga, Y. Nishida, M. Asobe, and A. J. Shields, "Efficient entanglement distribution over 200 kilometers," *Opt. Express* **17**, 11440–11449 (2009).
 36. T. Inagaki, N. Matsuda, O. Tadanaga, M. Asobe, and H. Takesue, "Entanglement distribution over 300 km of fiber," *Opt. Express* **21**, 23241–23249 (2013).
 37. D. Cozzolino, E. Polino, M. Valeri, G. Carvacho, D. Bacco, N. Spagnolo, L. K. K. Oxenlowe, and F. Sciarrino, "Air-core fiber distribution of hybrid vector vortex-polarization entangled states," *Adv. Photon.* **1**, 046005 (2019).
 38. J. Yin, Y. Cao, Y. H. Li, *et al.*, "Satellite-based entanglement distribution over 1200 kilometers," *Science* **356**, 1140–1144 (2017).
 39. R. Bedington, J. M. Arrazola, and A. Ling, "Progress in satellite quantum key distribution," *npj Quantum Inf.* **3**, 30 (2017).
 40. J.-G. Ren, P. Xu, H.-L. Yong, *et al.*, "Ground-to-satellite quantum teleportation," *Nature* **549**, 70–73 (2017).
 41. J. Yin, Y.-H. Li, S.-K. Liao, *et al.*, "Entanglement-based secure quantum cryptography over 1,120 kilometres," *Nature* **582**, 501–505 (2020).
 42. J. Pearl, *Causality* (Cambridge University, 2009).
 43. C. J. Wood and R. W. Spekkens, "The lesson of causal discovery algorithms for quantum correlations: causal explanations of Bell-inequality violations require fine-tuning," *New J. Phys.* **17**, 033002 (2015).
 44. R. Chaves, R. Kueng, J. B. Brask, and D. Gross, "Unifying framework for relaxations of the causal assumptions in Bell's theorem," *Phys. Rev. Lett.* **114**, 140403 (2015).
 45. C. Branciard, N. Gisin, and S. Pironio, "Characterizing the nonlocal correlations created via entanglement swapping," *Phys. Rev. Lett.* **104**, 170401 (2010).
 46. C. Branciard, D. Rosset, N. Gisin, and S. Pironio, "Bilocal versus non-bilocal correlations in entanglement-swapping experiments," *Phys. Rev. A* **85**, 032119 (2012).
 47. A. Tavakoli, N. Gisin, and C. Branciard, "Bilocal Bell inequalities violated by the quantum elegant joint measurement," *Phys. Rev. Lett.* **126**, 220401 (2021).
 48. M.-O. Renou, D. Trillo, M. Weilenmann, T. P. Le, A. Tavakoli, N. Gisin, A. Acin, and M. Navascués, "Quantum theory based on real numbers can be experimentally falsified," *Nature* **600**, 625–629 (2021).
 49. R. Chaves, C. Majenz, and D. Gross, "Information-theoretic implications of quantum causal structures," *Nat. Commun.* **6**, 5766 (2015).
 50. A. Tavakoli, P. Skrzypczyk, D. Cavalcanti, and A. Acn, "Nonlocal correlations in the star-network configuration," *Phys. Rev. A* **90**, 062109 (2014).
 51. R. Chaves, "Polynomial Bell inequalities," *Phys. Rev. Lett.* **116**, 010402 (2016).
 52. M.-O. Renou, E. Bäumer, S. Boreiri, N. Brunner, N. Gisin, and S. Beigi, "Genuine quantum nonlocality in the triangle network," *Phys. Rev. Lett.* **123**, 140401 (2019).
 53. T. Fritz, "Beyond Bell's theorem II: scenarios with arbitrary causal structure," *Commun. Math. Phys.* **341**, 391–434 (2016).
 54. J. Henson, R. Lal, and M. F. Pusey, "Theory-independent limits on correlations from generalized Bayesian networks," *New J. Phys.* **16**, 113043 (2014).
 55. E. Wolfe, R. W. Spekkens, and T. Fritz, "The inflation technique for causal inference with latent variables," *J. Causal Inference* **7**, 20170020 (2019).
 56. N. Gisin, "Entanglement 25 years after quantum teleportation: testing joint measurements in quantum networks," *Entropy* **21**, 325 (2019).
 57. A. Tavakoli, A. Pozas-Kerstjens, M.-X. Luo, and M.-O. Renou, "Bell non-locality in networks," *Rep. Prog. Phys.* **85**, 056001 (2022).
 58. G. Carvacho, F. Andreoli, L. Santodonato, M. Bentivegna, R. Chaves, and F. Sciarrino, "Experimental violation of local causality in a quantum network," *Nat. Commun.* **8**, 14775 (2017).
 59. D. J. Saunders, A. J. Bennet, C. Branciard, and G. J. Pryde, "Experimental demonstration of nonbilocal quantum correlations," *Sci. Adv.* **3**, e1602743 (2017).
 60. F. Andreoli, G. Carvacho, L. Santodonato, M. Bentivegna, R. Chaves, and F. Sciarrino, "Experimental bilocality violation without shared reference frames," *Phys. Rev. A* **95**, 062315 (2017).
 61. Q.-C. Sun, Y.-F. Jiang, B. Bai, W. Zhang, H. Li, X. Jiang, J. Zhang, L. You, X. Chen, Z. Wang, Q. Zhang, J. Fan, and J.-W. Pan, "Experimental demonstration of non-bilocality with truly independent sources and strict locality constraints," *Nat. Photonics* **13**, 687–691 (2019).
 62. D. Poderini, I. Agresti, G. Marchese, E. Polino, T. Giordani, A. Suprano, M. Valeri, G. Milani, N. Spagnolo, G. Carvacho, R. Chaves, and F. Sciarrino, "Experimental violation of n -locality in a star quantum network," *Nat. Commun.* **11**, 2467 (2020).
 63. R. Chaves, G. Carvacho, I. Agresti, V. Di Giulio, L. Aolita, S. Giacomini, and F. Sciarrino, "Quantum violation of an instrumental test," *Nat. Phys.* **14**, 291–296 (2018).
 64. E. Polino, I. Agresti, D. Poderini, G. Carvacho, G. Milani, G. B. Lemos, R. Chaves, and F. Sciarrino, "Device-independent test of a delayed choice experiment," *Phys. Rev. A* **100**, 022111 (2019).
 65. G. Carvacho, R. Chaves, and F. Sciarrino, "Perspective on experimental quantum causality," *Europhys. Lett.* **125**, 30001 (2019).
 66. M. Ringbauer, C. Giarmatzi, R. Chaves, F. Costa, A. G. White, and A. Fedrizzi, "Experimental test of nonlocal causality," *Sci. Adv.* **2**, e1600162 (2016).
 67. I. Agresti, D. Poderini, B. Polacchi, N. Miklin, M. Gachechiladze, A. Suprano, E. Polino, G. Milani, G. Carvacho, R. Chaves, and F. Sciarrino, "Experimental test of quantum causal influences," *Sci. Adv.* **8**, eabm1515 (2022).
 68. H. J. Kimble, "The quantum internet," *Nature* **453**, 1023–1030 (2008).
 69. M. Zukowski, A. Zeilinger, M. A. Horne, and A. K. Ekert, "Event-ready-detectors' Bell experiment via entanglement swapping," *Phys. Rev. Lett.* **71**, 4287 (1993).
 70. M. Zukowski, A. Zeilinger, and H. Weinfurter, "Entangling photons radiated by independent pulsed sources," *Ann. N.Y. Acad. Sci.* **755**, 91–102 (1995).
 71. N. Lütkenhaus, J. Calsamiglia, and K.-A. Suominen, "Bell measurements for teleportation," *Phys. Rev. A* **59**, 3295 (1999).
 72. L. Vaidman and N. Yoran, "Methods for reliable teleportation," *Phys. Rev. A* **59**, 116 (1999).
 73. F. Basso Basset, F. Salusti, L. Schweickert, M. B. Rota, D. Tedeschi, S. F. Covre da Silva, E. Roccia, V. Zwiller, K. D. Jöns, A. Rastelli, and R. Trotta, "Quantum teleportation with imperfect quantum dots," *npj Quantum Inf.* **7**, 7 (2021).
 74. M.-C. Chen, C. Wang, F.-M. Liu, J.-W. Wang, C. Ying, Z.-X. Shang, Y. Wu, M. Gong, H. Deng, F. Liang, Q. Zhang, C.-Z. Peng, X. Zhu, A. Cabello, C.-Y. Lu, and J.-W. Pan, "Ruling out real-valued standard formalism of quantum theory," *Phys. Rev. Lett.* **128**, 040403 (2022).
 75. D. Wu, Y.-F. Jiang, X.-M. Gu, L. Huang, B. Bai, Q.-C. Sun, S.-Q. Gong, Y. Mao, H.-S. Zhong, M.-C. Chen, J. Zhang, Q. Zhang, C.-Y. Lu, and J.-W. Pan, "Experimental refutation of real-valued quantum mechanics under strict locality conditions," arXiv:2201.04177 (2022).
 76. M. D. Eisaman, J. Fan, A. Migdall, and S. V. Polyakov, "Invited review article: single-photon sources and detectors," *Rev. Sci. Instrum.* **82**, 071101 (2011).
 77. S. Slussarenko, M. M. Weston, H. M. Chrzanowski, L. K. Shalm, V. B. Verma, S. W. Nam, and G. J. Pryde, "Unconditional violation of the shot-noise limit in photonic quantum metrology," *Nat. Photonics* **11**, 700–703 (2017).
 78. N. Lütkenhaus and M. Jähma, "Quantum key distribution with realistic states: photon-number statistics in the photon-number splitting attack," *New J. Phys.* **4**, 44 (2002).
 79. D. Huber, M. Reindl, S. F. Covre Da Silva, C. Schimpf, J. Martín-Sánchez, H. Huang, G. Piredda, J. Edlinger, A. Rastelli, and R. Trotta, "Strain-tunable GaAs quantum dot: a nearly dephasing-free source of entangled photon pairs on demand," *Phys. Rev. Lett.* **121**, 033902 (2018).
 80. S. Pironio, V. Scarani, and T. Vidick, "Focus on device independent quantum information," *New J. Phys.* **18**, 100202 (2016).

81. U. Vazirani and T. Vidick, "Fully device independent quantum key distribution," *Commun. ACM* **62**, 133 (2019).
82. V. Scarani, "The device-independent outlook on quantum physics," *Acta Phys. Slovaca* **62**, 347–409 (2012).
83. D. Poderini, E. Polino, G. Rodari, A. Suprano, R. Chaves, and F. Sciarrino, "*Ab initio* experimental violation of Bell inequalities," *Phys. Rev. Res.* **4**, 013159 (2022).
84. R. Arnon-Friedman, F. Dupuis, O. Fawzi, R. Renner, and T. Vidick, "Practical device-independent quantum cryptography via entropy accumulation," *Nat. Commun.* **9**, 459 (2018).
85. J. Ahrens, P. Badziag, A. Cabello, and M. Bourennane, "Experimental device-independent tests of classical and quantum dimensions," *Nat. Phys.* **8**, 592–595 (2012).
86. It is a particular case of the more general scheme, the star-shaped network [50,62,97 [Fig. 1(c)]. In this kind of network, n -nodes are connected to a central one, which is $n = 2$ for the bilocal case.
87. D. Rosset, C. Branciard, T. J. Barnea, G. Putz, N. Brunner, and N. Gisin, "Nonlinear Bell inequalities tailored for quantum networks," *Phys. Rev. Lett.* **116**, 010403 (2016).
88. N. Gisin, Q. Mei, A. Tavakoli, M. O. Renou, and N. Brunner, "All entangled pure quantum states violate the bilocality inequality," *Phys. Rev. A* **96**, 020304 (2017).
89. F. Andreoli, G. Carvacho, L. Santodonato, R. Chaves, and F. Sciarrino, "Maximal qubit violation of n -locality inequalities in a star-shaped quantum network," *New J. Phys.* **19**, 113020 (2017).
90. J. F. Clauser, M. A. Horne, A. Shimony, and R. A. Holt, "Proposed experiment to test local hidden-variable theories," *Phys. Rev. Lett.* **23**, 880 (1969).
91. S. F. Covre da Silva, G. Undeutsch, B. Lehner, S. Manna, T. M. Krieger, M. Reindl, C. Schimpf, R. Trotta, and A. Rastelli, "GaAs quantum dots grown by droplet etching epitaxy as quantum light sources," *Appl. Phys. Lett.* **119**, 120502 (2021).
92. F. Basso Basset, M. B. Rota, C. Schimpf, D. Tedeschi, K. D. Zeuner, S. F. Covre da Silva, M. Reindl, V. Zwiller, K. D. Jöns, A. Rastelli, and R. Trotta, "Entanglement swapping with photons generated on demand by a quantum dot," *Phys. Rev. Lett.* **123**, 160501 (2019).
93. H. Jayakumar, A. Predojević, T. Huber, T. Kauten, G. S. Solomon, and G. Weihs, "Deterministic photon pairs and coherent optical control of a single quantum dot," *Phys. Rev. Lett.* **110**, 135505 (2013).
94. D. S. Hum and M. M. Fejer, "Quasi-phasematching," *C. R. Physique* **8**, 180–198 (2007).
95. S. Popescu and D. Rohrlich, "Quantum nonlocality as an axiom," *Found. Phys.* **24**, 379–385 (1994).
96. T. Huber, M. Prilmüller, M. Sehner, G. S. Solomon, A. Predojević, and G. Weihs, "Interfacing a quantum dot with a spontaneous parametric down-conversion source," *Quantum Sci. Technol.* **2**, 034016 (2017).
97. E. Bäumer, N. Gisin, and A. Tavakoli, "Demonstrating the power of quantum computers, certification of highly entangled measurements and scalable quantum nonlocality," *npj Quantum Inf.* **7**, 117 (2021).